



This is a repository copy of *Role of configurational entropy in body-centred cubic or face-centred cubic phase formation in high entropy alloys*.

White Rose Research Online URL for this paper:
<http://eprints.whiterose.ac.uk/102378/>

Version: Accepted Version

Article:

Anand, G., Goodall, R. and Freeman, C.L. (2016) Role of configurational entropy in body-centred cubic or face-centred cubic phase formation in high entropy alloys. *Scripta Materialia*, 124. pp. 90-94. ISSN 1359-6462

<https://doi.org/10.1016/j.scriptamat.2016.07.001>

Article available under the terms of the CC-BY-NC-ND licence
(<https://creativecommons.org/licenses/by-nc-nd/4.0/>)

Reuse

This article is distributed under the terms of the Creative Commons Attribution-NonCommercial-NoDerivs (CC BY-NC-ND) licence. This licence only allows you to download this work and share it with others as long as you credit the authors, but you can't change the article in any way or use it commercially. More information and the full terms of the licence here: <https://creativecommons.org/licenses/>

Takedown

If you consider content in White Rose Research Online to be in breach of UK law, please notify us by emailing eprints@whiterose.ac.uk including the URL of the record and the reason for the withdrawal request.



eprints@whiterose.ac.uk
<https://eprints.whiterose.ac.uk/>

Role of configurational entropy in body-centred cubic or face-centred cubic phase formation in high entropy alloys

G. Anand^{a*}, R. Goodall^a, Colin L. Freeman^a

^aDepartment of Materials Science and Engineering, University of Sheffield, Sheffield S1 3JD

*E-mail: ganand1@sheffield.ac.uk

Tel: +44(0)114 222 5998; Fax: +44(0)114 222 5943

Abstract

This study examines the comparative phase stability of transition and late transition element based high entropy alloys in body-centred cubic (BCC) or face-centred cubic (FCC) forms using a combined classical molecular dynamics and statistical mechanics based approach. Multi-configurational sampling was carried out using a hybrid genetic algorithm-molecular dynamics (GA-MD) based method. The calculations demonstrate that comparative BCC or FCC phase stability is influenced by configurational entropy. The present study also provides a theoretical explanation of the recently reported occurrence of BCC phase in CoCrFeNi HEA, where the high temperature structure may be retained.

Keywords: High entropy alloys, Phase transformations, Molecular Dynamics (MD), Statistical mechanics, Thermodynamics.

High entropy alloys (HEAs) are a class of multicomponent metallic alloys [1], which exhibit simple crystal structures such as body-centred cubic (BCC), face-centred cubic (FCC), hexagonal cubic phase (HCP) or orthorhombic [2-4] crystal structures. The stabilisation of a solid solution phase over intermetallic and amorphous alloy formation in such multicomponent systems was initially attributed to the high configurational entropy of mixing [5]. The prediction of the comparative phase stability of BCC and FCC phases for HEAs remains a major debate in the literature. For example, CoCrFeNi shows the FCC structure [6], but addition of Al causes its transformation to the BCC crystal structure [6]. The phase transformation and existence of HEAs in two main types of crystal structures was initially rationalised in terms of the conventional metallurgical concept of FCC and BCC stabilising elements [7]. Traditionally, phase stability in alloys has been understood in terms of the number of electrons per atom (e/a) [8], which has been extensively used for Hume-Rothery electron phase stabilisation. In the case of HEA, which are mostly composed of transition metals, the accurate determination of the e/a ratio is problematic. Hence, the valence electron concentration (VEC) has been employed to rationalise FCC and BCC formation, where higher VEC (≥ 8.0) leads to FCC phases, while lower VEC (≤ 6.87) causes BCC formation, leaving a mixture of BCC and FCC phase for $6.87 \leq \text{VEC} \leq 8.0$ [9]. This criterion, however, does not apply to HEA containing Mn [10], and in certain cases the effect of cooling conditions dominates the phase formation, i.e., alloys with the same

composition but subjected to different processing conditions produce different phase occurrence characteristics [11]. Therefore phase selection remains an open debate. Computationally expensive *ab-initio* approaches, such as coherent potential approximation [12] and special quasi-random structures with density functional theory (DFT) [13] have been used to study HEAs. Given the potential significance of (configurational) entropy in the phase stability in HEAs, there is a need for an extensive sampling of configurations, which cannot be achieved easily with *ab-initio* methods that are limited to small cells. The present study attempts to address this issue by using atomistic simulation with a genetic algorithm (GA) as the sampling strategy followed by a statistical mechanics technique for the calculation of the configurational entropy.

The DL_POLY code was employed to carry out Molecular Dynamics (MD) simulations [14]. Position, velocity and acceleration of the atoms were updated via the velocity-verlet integration algorithm [15]. The GULP code [16] was used to generate 7x7x7 (FCC) and 9x9x9 (BCC) cubic supercells for starting configurations. The disordered structures of the alloys were generated by randomising the elements on the lattice sites. The simulations were performed with a 1 fs time-step. The long-range interaction cut-off was set to be 6 Å. The MD simulations were carried out for 10 ps, where the system was equilibrated for first 5000 time steps. The configurational energy was shown to converge over this time (see Fig. A1 in supplementary information). A N ose-Hoover NPT ensemble with thermostat and barostat relaxation times of 0.01 ps and 0.1 ps, respectively, was used to keep temperature (300 K) and pressure (1 atmosphere) constant. The initial lattice parameters for the BCC and the FCC variant of AlCoCrFeNi, CoCrFeNi and CoCrFeNiTi were taken from first-principle calculations, while for Al_{0.5}CoCrFeNi, the equilibrium lattice parameter was calculated from finding the minimum of the energy-volume curve in NVT calculation. The initial lattice parameters used in MD simulations are tabulated in Table A1 in the supplementary information.

The embedded atom method (EAM) potential for elements (Al, Co, Fe, Ni and Ti) were taken from Zhou *et. al.* [17] and the interatomic potentials of Cr was taken Lin *et. al.* [18]. Although, Lin *et. al.* used a similar parameter model as of Zhou *et. al.*, it was found that the parameterisation followed a different rule-set. This resulted in substantial instabilities in the alloys. Therefore, the Cr potential was modified as per ref. [17] (detailed discussion can be found in supplementary information)

Initially, MD calculations on the 2500 randomly generated configurations of each alloy were carried out. It was noticed that energy distribution of these randomly generated configurations did not necessarily follow the Maxwell-Boltzmann distribution suggesting that our distribution did not include many important lower energy configurations. This provided the motivation for the development of the hybrid GA-MD based methodology to ensure the sampling low energy configurations.

The systematic generation of a new configuration of atoms on the lattice is two-step process, as represented schematically in Fig.1. In the first step, the swapping is carried out between two supercells (Parent-1 and Parent-2) at the same equivalent position (so that child-1 and child-2 inherit certain atomic positions from parent-1 and parent-2 respectively). In next step, the constant composition of the supercell is maintained by the swapping of random positions. This process is repeated randomly for 10-30% of the total number of atoms in the supercell. These children are then used as input configurations for MD simulations. After these simulations are completed the new configurations act as parent configurations for the next generation etc. The selection of parents is performed with reference to their energy, with the probability of selection for a low energy configuration higher than high-energy configurations. This process represents the iterative cycle of two-step swapping-MD calculation-selection of configurations.

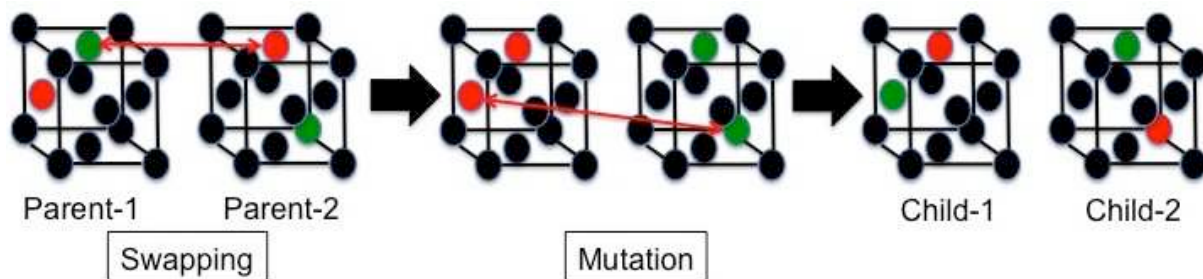


Figure 1: Schematic representation of two-step swapping process for generation of new configurations.

It is important to note that, once the energy variation in the population had reached zero (all configurations had the same energy) and the thermodynamic values (such as enthalpy and entropy) had reached a constant value, then further sampling was unlikely to improve the population in terms of finding lower energy configurations. Therefore, this provided the rationalisation to stop the GA-MD cycle.

Figure 2(a) shows that 61 and 71 generations of GA-MD cycle are required for BCC and FCC variants of $\text{Al}_{0.5}\text{CoCrFeNi}$ are required to reach the state, when all the configurations have equal energy. For AlCoCrFeNi , the BCC and FCC phases both required 77 cycles. For BCC- CoCrFeNi , 71 generations were required, while 82 cycles were required for the FCC variant. 55 and 56 generations were required for BCC and FCC variants of CoCrFeNiTi , respectively (a pictorial representation of these data can be found in the supplementary material). It should be noted that the BCC variant reaches the state when all the configurations have same energy before the FCC variants in all the cases, which is surprising since the number of atoms simulated in the BCC (1458 atoms) was slightly higher than the FCC (1372 atoms).

Thermodynamic quantities such as, enthalpy (H) and Gibbs free energy (G) were calculated using the configurational energy (E_i) of the atomic configurations, i . H can be calculated using equation (1) as:

$$H = \frac{\sum_{i=1}^N E_i \exp\left(\frac{-E_i}{k_B T}\right)}{\sum_{i=1}^N \exp\left(\frac{-E_i}{k_B T}\right)} \quad (1)$$

Where N in equation (1) represents the total number of atomic configurations sampled. k_B and T are the Boltzmann constant and temperature respectively.

G can similarly be calculated using equation (2), as:

$$G = -k_B T \cdot \ln \sum_{i=1}^N \exp\left(\frac{-E_i}{k_B T}\right) \quad (2)$$

It should be noted that, as the GA-MD cycle progresses with each generation, the energy values of configurations generated in that particular generation and energy values from prior generations are used to calculate the thermodynamic quantities. Therefore as the GA-MD cycle progresses, we are adding further configurations to the thermodynamic average.

With the knowledge of H and G , the entropy (S_{calc}) can be calculated using equation (3), as:

$$S_{calc} = \frac{H - G}{T} \quad (3)$$

The upper limit of S , i.e., S_{id} is additionally calculated for comparison using equation (4), as:

$$S_{id} = y \cdot \ln(y) - \sum_{i=1}^K x_i \cdot \ln(x_i) \left(\text{where, } y = \sum_{i=1}^K x_i \right) \quad (4)$$

where, y in above equation represents the total number of atoms in the supercell, K is total number of element in the alloy and x_i is number of i^{th} element.

The influence of the number of generations on thermodynamic properties such as enthalpy (H) and entropy (S_{calc}) was studied and is presented for $Al_{0.5}CoCrFeNi$ in Fig. 2 (b) and (c), respectively (H and S_{calc} variations for other HEA systems are presented in supplementary material). It should be noted at this point that thermodynamic parameters are calculated to observe the convergence in GA-MD cycle. Once the GA-MD cycle is complete, it provides the available energy states, which can be used to calculate the bulk thermodynamic properties through Boltzmann framework.

The enthalpy of mixing (H_{mix}) was calculated for the alloys using equation (5). The H value for the BCC variant of $Al_{0.5}CoCrFeNi$, is calculated using equation (1) using energy values until 61 generations were reached for this particular case.

$$H_{mix} = y \cdot H - \sum_{k=1}^K n_k \cdot E_k \quad (5)$$

where, K is the number of the elements in the alloy, n_k is the number of and E_k is the configurational energy of the k^{th} element in alloy mix (Table A4 in supplementary information). A similar procedure was followed for other the HEAs and the H_{mix} are shown in Table 1. H_{mix} values for all HEA, excluding BCC-CoCrFeNiTi, are in the $-0.228 \leq H_{mix} \leq 0.073$ eV/atom range, defined empirically for HEAs [19]. This implies that some HEAs are potentially stabilised through both enthalpic as well as entropic contributions. It is also important to note that the BCC phase has a lower H_{mix} compared to the FCC phase in all cases. This suggests a possible limitation of the EAM potential used in the present investigation; however, it does not indicate that the relative energies within each phase are not reliable which controls the configurational entropy.

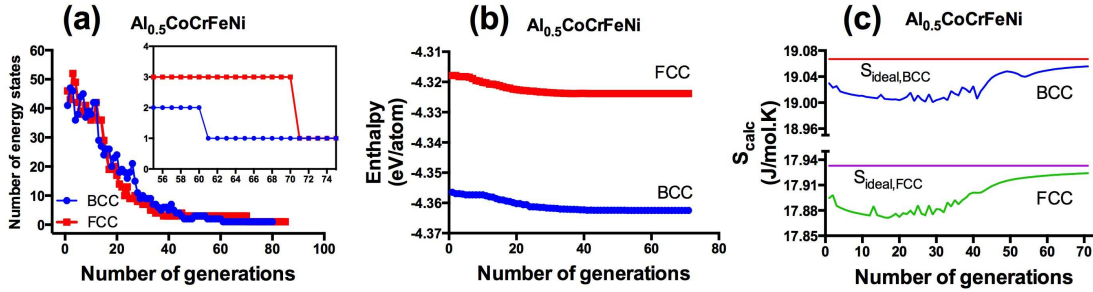


Figure 2 (a): Number of energy states with an unique value, (b) enthalpy and (c) entropy with successive GA-MD cycle.

Alloy	H_{mix} (eV/atom)	
	BCC	FCC
Al _{0.5} CoCrFeNi	-0.1244	-0.0849
AlCoCrFeNi	-0.1738	-0.1354
CoCrFeNi	-0.0560	-0.0168
CoCrFeNiTi	-0.2654	-0.2291

Table 1: Enthalpy of mixing values for different HEA.

The probability of the occurrence of a particular energy state (P_i) can be calculated from equation (6) [20], as:

$$P_i = \frac{\exp\left(\frac{-E_i}{k_B T}\right)}{\sum_{i=1}^N \exp\left(\frac{-E_i}{k_B T}\right)} \quad (6)$$

Where N in equation (6) represents the number of energy states sampled (e.g. all the energy states from 61 generations of GA-MD cycle for $\text{Al}_{0.5}\text{CoCrFeNi}$). The configurational entropy (S_{conf}) can then be calculated from the probability of occurrence (P_i) of particular energy state (E_i), using equation (7), as:

$$S_{conf} = -k_B \sum_{i=1}^z P_i \ln(P_i) \quad (7)$$

where, z represents the number of energy states having non-zero probability of occurrence. Figure 3 shows the configurational entropy for different HEAs at 300 K. The FCC phase has higher configurational entropy in comparison with the BCC phase for $\text{Al}_{0.5}\text{CoCrFeNi}$, CoCrFeNi and CoCrFeNiTi at 300K. While the BCC phase has higher configurational entropy in comparison to the FCC phase for AlCoCrFeNi . It should be noted that the FCC is the stable crystal structure for $\text{Al}_{0.5}\text{CoCrFeNi}$ [21], CoCrFeNi [22] and CoCrFeNiTi [23], while AlCoCrFeNi exhibits the BCC crystal structure [24]. This implies that the configurational entropy might be playing crucial role in phase selection.

The effect of temperature on the S_{conf} is shown in Figure 4. As mentioned before the BCC systems tend to reach the state of zero variation in energy earlier than their FCC counterparts. Hence, it is an important point of consideration while calculating S_{conf} , how many energy states should be included? In the present case for BCC; two sets of energy states were considered. In the first case, all configurations were included until the energy values from the GA-MD run had reached the state of zero variation in energy (as shown previously), while in the later case, the number of generations for GA-MD cycle was kept equal to the number of generations required for the FCC phase (and therefore run for longer). As can be seen from Figure 4, allowing the GA-MD cycle for BCC systems to run for an equal number of generations as for the FCC, leads to upward shift in the curve (and hence an increase in the configurational entropy), as more energy states are available to the system. It can be seen from Fig. 4, that in the case of $\text{Al}_{0.5}\text{CoCrFeNi}$ and CoCrFeNiTi , the FCC phases still have a higher configurational entropy than the BCC phase throughout the temperature range, while in the case of AlCoCrFeNi , the BCC phase remains entropically favourable. For CoCrFeNi , when the energy states from a number of equal GA-MD generations are considered, the FCC phase still has a higher configurational entropy than the BCC at low temperatures, but the reverse is true at higher temperatures. This observation provides a potential explanation for recent experimental findings of the BCC phase in CoCrFeNi supercooled from high temperature [25] and during mechanical alloying [26]. It is also important to note that in the case of AlCoCrFeNi , the S_{conf} for BCC shows a decreasing trend of 8.355 to 8.286 k_B/atom , when the temperature is varied from 100 K to 1500 K. In comparison, S_{conf} for FCC- AlCoCrFeNi continuously increases from 7.462 to 8.007 k_B/atom . Even though, we do not observe inflection between BCC and FCC phases for AlCoCrFeNi , it does provide

the qualitative explanation of the small amount the FCC phase in AlCoCrFeNi, as observed experimentally [6]. Additionally, it can be seen in the case of CoCrFeNiTi, the S_{conf} is lower in comparison with the Al_{0.5}CoCrFeNi, AlCoCrFeNi and CoCrFeNi, which can be understood in terms of propensity of this alloy system to have intermetallic phases in the as-cast state.

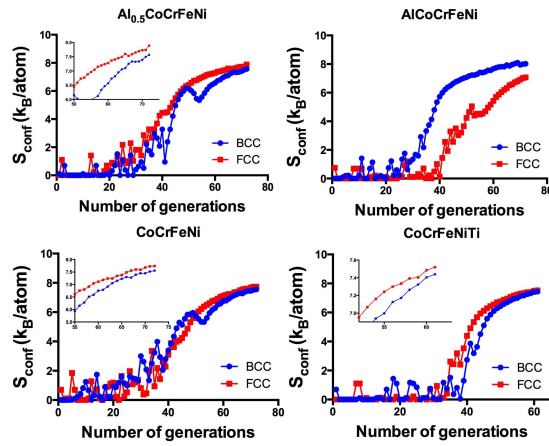


Figure 3: The configurational entropy of BCC and FCC variants of HEA with number of generations of GA-MD cycle at 300 K.

It is clear from recent reports that HEAs are kinetically stabilised solid solutions in simple crystal structure [27-29] and the comparative phase stability is influenced by the processing methods [30]. Hence, the present investigation provides evidence that configurational entropy might be playing crucial role in that phase selection, particularly in non-equilibrium processing routes in certain HEAs.

In summary, this study provides a methodology for sampling these disordered systems through a hybrid GA-MD framework and a theoretical explanation for BCC and FCC phase formation in HEAs. It has been shown that comparative phase stability may be governed by the configurational entropy of the phase. Additionally, the variation in entropy with temperature provides an explanation for the occurrence of the BCC phase in CoCrFeNi alloy, which mostly exhibits the FCC phase. The same approach provides an explanation of the occurrence of the minor concentration FCC phase in AlCoCrFeNi HEA.

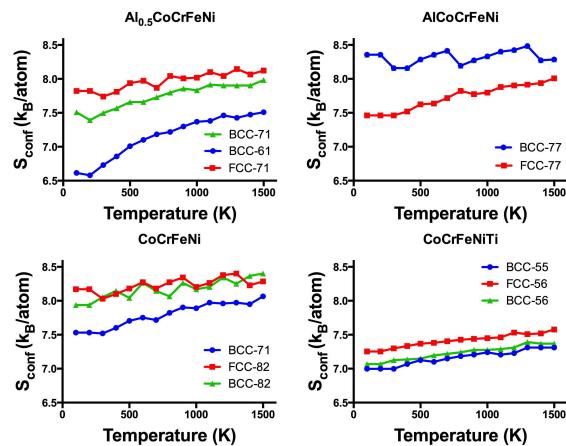


Figure 4: The variation of configurational entropy with temperature.

The authors are thankful for support provided via our membership of the UK's HEC Materials Chemistry Consortium, which is funded by EPSRC (EP/L000202). GA is thankful to University of Sheffield for PhD scholarship.

References

1. B. Cantor, I.T.H. Chang, P. Knight, A.J.B. Vincent, *Mater. Sci. Eng. A*. 375-377 (2004) 213-218.
2. Y. Zhang, T.T. Zuo, Z. Tang, M.C. Gao, K.A. Dahmen, P.K. Liaw, and Z.P. Lu, *Prog. Mater. Sci.* 61 (2014) 1-93.
3. A. Takeuchi, K. Amiya, T. Wada, K. Yubuta, W. Zhang, *JOM*. 66 (2014) 1984-1992.
4. L. Liliensten, J.P. Couzinie, L. Perriere, J. Bourgon, N. Emery, I. Guillot, *Mater. Lett.* 32 (2014) 123-125.
5. J.W. Yeh, S.K. Chen, S.J. Lin, J.Y. Gan, T.S. Chin, T.T. Shun, C. H. Tsau, S. Y. Chang, *Adv. Eng. Mater.* 6 (2004) 299-303.
6. H.P. Chou, Y.S. Chang, S.K. Chen, J.W. Yeh, *Mater. Sci. Eng. B*. 163 (2009) 184-189.
7. Guan-Yu Ke, Swe-Kai Chen, Tung Hsu, Jien-Wei Yeh, *Annales De Chimie – Science des Materiaux*. 31(2006) 669-684.
8. U. Mizutani, *Hume–Rothery rules for structurally complex alloy phases*, CRC Press, Boca Raton, 2011.
9. S. Guo, C. Ng, J. Lu, C. T. Liu, *J. Appl. Phys.* 109 (2011) 103505.
10. S. Guo, *Mater. Sci. Tech.* 31 (2015) 1223-1230.
11. S. Singh, N. Wanderka, B. S. Murty, U. Glatzel, J. Banhart, *Acta. Mater.* 59 (2011) 182-190.
12. F. Tian, L. Varga, N. Chen, L. Delczeg, L. Vitos, *Phys. Rev. B*. 87 (7) (2013) 075144.
13. A.J. Zaddach, C. Niu, C.C. Koch, D.L. Irving, *JOM*. 65 (2013) 1780-1789.
14. W. Smith and T.R. Forester, *J. Mol. Graphics*. 198/199 (1996) 796-781.

15. M. P. Allen and D. J. Tindesley, *Simulation of Liquids*, Clarendon Press, Oxford, 1989.
16. J. D. Gale, *JCS Faraday Trans*, 93 (1997) 629-637.
17. X.W. Zhou, H.N.G. Wadley, R.A. Johnson, D.J. Larson, N. Tabet, A. Cerezo, A.K. Petford-Long, G.D.W. Smith, P.H. Clifton, R.L. Martens, T.F. Kelly, *Acta Mater.* 49 (2001) 4005-4015.
18. Z.A. Lin, R.A. Johnson, L.V. Zhigilei, *Phys. Rev B.* 77 (2008) 214108.
19. S. Guo and C.T. Liu, *Progress in Natural Science: Materials International* 21 (2011) 433-446.
20. R. Grau-Crespo, U.V. Waghmare, *Simulation of crystals with chemical disorder at lattice sites*, in: Bina Rai (Ed.), *Molecular modelling for design of novel performance chemicals and materials*, CRC presss, Boca Raton, 2012, pp. 303-326.
21. C. M. Lin, H.L. Tsai, *Intermetallics.* 19 (2011) 288-294.
22. Y. Brif, M. Thomas, I. Todd, *Scripta Mater.* 99 (2015) 93-96.
23. K.B. Zhang, Z.Y. Fu, J.Y. Zhang, W.M. Wang, H. Wang, Y.C. Wang, Q.J. Zhang, J. Shi, *Mater Sci Eng A.* 508(2009) 214-219.
24. W.R. Wang, W.L. Wang, S.C. Wang, Y.C. Tsai, C.H. Lai, J.W. Yeh, *Intermetallics.* 26 (2012) 44-51.
25. J. Li, W. Jia, J. Wang, H. Kou, D. Zhang, E. Beaugnon, *Mater. & Des.* 95 (2016) 183-187.
26. S. Praveen, B.S. Murty, R.S. Kottada, *Mater Sci Eng A.* 534 (2012) 83-89.
27. D. Ma, M. Yao, K.G. Pradeep, C.C. Tasan, H. Springer, D. Raabe, *Acta Mater.* 98 (2015) 288-296.
28. E.J. Pickering, R. Munoz-Moreno, H.J. Stone, N.G. Jones, *Scripta Mater.* 113 (2016) 106-109.
29. F. Otto, A. Dlouhy, K.G. Pradeep, M. Kubenova, D. Raabe, G. Eggler, E.P. George, *Acta Mater.* 112 (2016) 40-52.
30. S.S. Ghazi, K.R. Ravi, *Intermetallics,* 73 (2016) 40-42.